Interference phenomena at backscattering by ice crystals of irregular shape

Alexander V. Konoshonkin[a,b], Natalia V. Kustova*[b], Anatoli G. Borovoi[a,b]
[a]National Research Tomsk State University, 36, Lenina Avenue, Tomsk, 634050, Russia;
[b]V.E. Zuev Institute of Atmospheric Optics, Rus. Acad. Sci., 1 Academician Zuev Sq., Tomsk, 634021, Russia.

ABSTRACT

It is shown that light backscattering by hexagonal ice crystals of cirrus clouds is formed by both diffraction and interference phenomena. Diffraction determines the angular width of the backscattering peak and interference produces the interference rings inside the peak. By use of a simplest model for distortion of the pristine hexagonal shape, we show that the shape distortion leads to both oscillations of the scattering (Mueller) matrix within the backscattering peak and to a strong increase of the depolarization, color, and lidar ratios needed for interpretation of lidar signals.

Keywords: physical optics, interference, light scattering, cirrus clouds

1. INTRODUCTION

Besides of great variance of sizes, shapes, and kind of spatial orientations of the ice crystals constituting cirrus clouds, a new item becomes recently a challenge for the scientific community dealing with optics of cirrus. Namely, it is suggested that ice crystal surfaces are not pristine [1-4] where imperfectness of the ice crystals is assumed to be double-natured. First, the dihedral angles inherent to the regular or pristine crystals can be scarcely distorted. This case is called the shape distortion. Second, every smooth face can be imagined as a sheet of rough surface whose spatial irregularities are less than the face size. This case is called the roughened crystals. A simplest numerical method taking into account the both kinds of imperfectness was proposed by Macke within his geometric-optics or ray-tracing code [5]. Here every ray reflected or refracted by a smooth face is artificially deviated from its geometric-optics propagation direction that is just associated with the crystal imperfectness. A drawback of this procedure is that it is not plausible from the physical point of view. To overcome this inconsistency, Liu et al. [6] recently applied the PSTD (pseudo-spectral time domain) method to a roughened hexagonal column where every roughened face was simulated numerically. However, this algorithm demands considerable computer resources and therefore it is restricted by crystals of moderate sizes. Later these authors compared the ice crystal optical properties obtained for the both models of the irregular crystals, i.e. the roughened and shape-distorted crystals, and concluded that the both models gave similar results [7].

Among all scattering directions, the backward direction is of special importance since it is only backscattering that is detected by lidars. In spite of a long history of studying cirrus clouds by means of lidars, the problem of backscattering by ice cloud crystals has not been clarified neither theoretically nor experimentally until now [8-23]. In particular, in the literature there is a discussion whether there is a sharp angular peak around the backward scattering direction in cirrus clouds. To answer the question, two methods, PSTD and invariant embedding T-matrix method, were recently applied by Zhou and Yang to a case of a randomly oriented hexagonal column of the size parameter of $a \approx 30$ [24]. They concluded that, for this crystal, the backscattering peak appeared always independently of the crystal was regular, roughened or shape-distorted. As for the regular hexagonal crystals, we showed within the geometric-optics approximation a long time ago [25,26] that the backscattering peak for the regular hexagonal columns and plates always appeared owing to the corner-reflector effect. Here the dihedral angle of 90° operates as a 2D corner-reflector. Later, within the framework of the physical-optics approximation, we showed [27] that the plane-parallel beams leaving a crystal in the backward direction are scattered owing to the Fraunhofer diffraction that just results in this backscattering peak. It is important to mention that the diffracted beams interfere with each other creating a quickly oscillating fine angular

*kustova@iao.ru; phone +7 3822 492864; fax +7 3822 492086; iao.ru

21st International Symposium on Atmospheric and Ocean Optics: Atmospheric Physics,
edited by G. G. Matvienko, O. A. Romanovskii, Proc. of SPIE Vol. 9680, 96802V
 · doi: 10.1117/12.2204872

structure inside the backscattering peak. In our recent paper [28], we calculated the scattering (Mueller) matrix corresponding to this fine angular structure for randomly oriented crystals of the regular shape.

Meanwhile, the angular width of the backscattering peak formed by cirrus clouds is too wide to be of interest for common monostatic lidars. The scattering matrix in the center of the peak, i.e. at exactly backward direction, is needed for interpretation of lidar signals. Here such three characteristics of lidar signals as depolarization, lidar and color ratios are of practical use. These characteristics were calculated by the authors [29] for the regular crystals of arbitrary orientation beginning from the horizontal up to random orientation. Owing to these calculations [28,29], we were able to ascertain that the ratios calculated for the regular crystals did not match well with the available experimental data. For example, the depolarization ratio calculated for the randomly oriented hexagonal columns was equal to about 0.2 while the typical experimental data were of about 0.5.

In this paper, we show that the interference phenomena taking place inside the backscattering peak prove to be very sensitive to crystal geometry. In particular, if the faces responsible for the corner-reflector effect, i.e. oriented at 90° to each other, are tilted a bit violating the angle 90°, this small tilt changes negligibly the total angular width of the backscattering peak but the interference pattern at the exact backward direction becomes significantly changed. As a result, the inconsistency between the experimental backscatter ratios and the quantities calculated for the hexagonal columns disappears if the crystals are irregularly shaped.

2. HEXAGONAL ICE COLUMNS OF REGULAR AND IRREGULAR SHAPES

The purpose of this paper is to clarify the main physical regularities appearing in optical properties of cirrus clouds because of small deviations of crystal surfaces from their regular or pristine shapes. We choose the hexagonal column as the basic shape since it is the typical shape of the crystals in cirrus clouds. Besides, it is the hexagonal column that is used in majority of the papers dealing with any test calculations of the optical properties. In this paper, we consider the hexagonal column of the typical diameter of $D = 30\,\mu\text{m}$. Heights of the columns h in cirrus clouds are not statistically independent of the diameters. The height is taken from the model of [30] as $h = 73.64\,\mu\text{m}$. The refractive index is taken as 1.3116 and 1.3004 for $\lambda = 0.532\,\mu\text{m}$ and $\lambda = 1.064\,\mu\text{m}$, respectively. The main axis is assumed to pass through centers of the hexagonal faces.

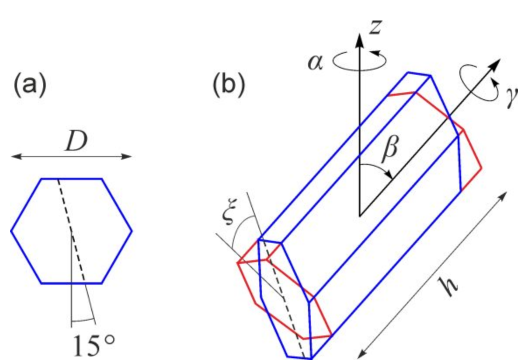

Figure 1. Geometry of the irregular hexagonal column.

The shape distortion of the column is defined by a simultaneous tilt of the both hexagonal faces relative to the main column axis. The tilt is chosen along the dashed line depicted in Fig. 1(a). Such distortion destroys all dihedral angles of 90° inside the crystal and excludes any plane of symmetry of the particle. The angle of the tilt ξ characterizes the surface distortion and it is called the distortion angle.

Orientation of a column is determined by three Euler angles α, β, and γ shown in Fig. 1(b) where α defines rotation of the crystal about the incident direction; β is the crystal tilt, i.e. the angle between the incident direction and the main axis; and γ describes crystal rotation about the main axis.

3. SCATTERING MATRICES AND BACKSCATTER RATIOS

In general, light scattering by an arbitrary particle is completely determined by the 4×4 scattering or Mueller matrix [31]. If a particle of arbitrary shape is randomly oriented, there are pairs of the so-called reciprocal particle orientations that reduce the number of independent elements of the Mueller matrix from 16 to 10 as follows

$$\mathbf{M}(\theta)=\sigma(\theta)\begin{pmatrix} 1 & m_{12}(\theta) & m_{13}(\theta) & m_{14}(\theta) \\ m_{12}(\theta) & m_{22}(\theta) & m_{23}(\theta) & m_{24}(\theta) \\ -m_{13}(\theta) & -m_{23}(\theta) & m_{33}(\theta) & m_{34}(\theta) \\ m_{14}(\theta) & m_{24}(\theta) & -m_{34}(\theta) & m_{44}(\theta) \end{pmatrix}. \tag{1}$$

The zenith scattering angle θ is counted, for convenience, from the backward scattering direction $\theta=0$. In Eq. (1), the first element of the matrix $M_{11}(\theta)=\sigma(\theta)$ has a simple physical meaning of the differential scattering cross section in the case of unpolarized incident light. Other dimensionless elements of the matrix $m_{ij}(\theta)$ are responsible for light polarization. If the particle has a plane of symmetry like the regular hexagonal column, four elements m_{13}, m_{14}, m_{23}, and m_{24} become zero.

Lidars detect only light scattered in the backward direction. For the backward direction $\theta=0$, the matrix is simplified as

$$\mathbf{M}(0)=\sigma(0)\begin{pmatrix} 1 & 0 & 0 & m_{14}(0) \\ 0 & m_{22}(0) & 0 & 0 \\ 0 & 0 & -m_{22}(0) & 0 \\ m_{14}(0) & 0 & 0 & 1-2m_{22}(0) \end{pmatrix}. \tag{2}$$

In lidar studies, three dimensionless ratios are often used instead of the Mueller matrix. They are

$$\delta_l=\frac{\sigma_\perp(0)}{\sigma_\parallel(0)},\quad L=\frac{\sigma_e}{\sigma(0)},\quad \chi=\frac{\sigma(0,\lambda_1)}{\sigma(0,\lambda_2)}. \tag{3}$$

The quantity δ_l is the linear depolarization ratio. It is obtained when the incident light is linearly polarized and the backscattering cross section is detected with the polarizer which is either perpendicular $\sigma_\perp(0)$ or parallel $\sigma_\parallel(0)$ to the incident light. The quantity L is called either the extinction-to-backscatter or lidar ratio. Here σ_e is the extinction cross section for the randomly oriented crystals that is calculated separately. The quantity χ is the color ratio which is detected by a two-wavelength lidar.

4. BACKSCATTERING PEAK FOR THE RANDOMLY ORIENTED IRREGULAR COLUMNS

Fig. 2 shows the differential scattering cross section $\sigma(\theta)$ for the randomly oriented regular and irregular columns calculated in both the geometric-optics and physical-optics approximations. Let us begin with the geometric-optics values. We see that the regular column creates the singularity like $1/\theta$ because of the corner-reflection effect as it was described in details earlier [4]. As for the irregular columns, it is obvious that at the fixed column orientation ($\beta\approx32°$, $\gamma=0°$) any shape distortion violating the dihedral angle of 90° shifts the scattering directions of all 8 beams from the backward direction $\theta=0$ to its vicinity $\theta\neq0$. Moreover, we proved that it was impossible to return the beams to the backward direction by a change of particle orientations. Therefore we watch in Fig. 2 that the shape distortion has replaced the singular peak of the backward direction by some regular functions $\sigma(\theta)$ which have a gap at the backward direction, the angular radius of this gap being about the distortion angle ξ.

In the physical-optics approximation, the geometric-optics gap and peaks have been smoothed as it is presented by the solid curves. We obtain that these curves distinctly reveal the backscattering or diffraction peak which outspreads roughly until the diffraction angle θ_d. Beyong the diffraction peak $\theta>\theta_d$, the geometric-optics and physical-optics functions $\sigma(\theta)$ practically approach each other. Thus, the backscattering peak of the angular radius of about θ_d exists for the shape-distorted crystals as well. However, the amplitude of this backscattering peak strongly decreases with the distortion angle ξ as seen in Fig. 2. As a result, we conclude that the backscattering peak practically disappears if the distortion angle exceeds the diffraction angle: $\xi > \theta_{dif}$.

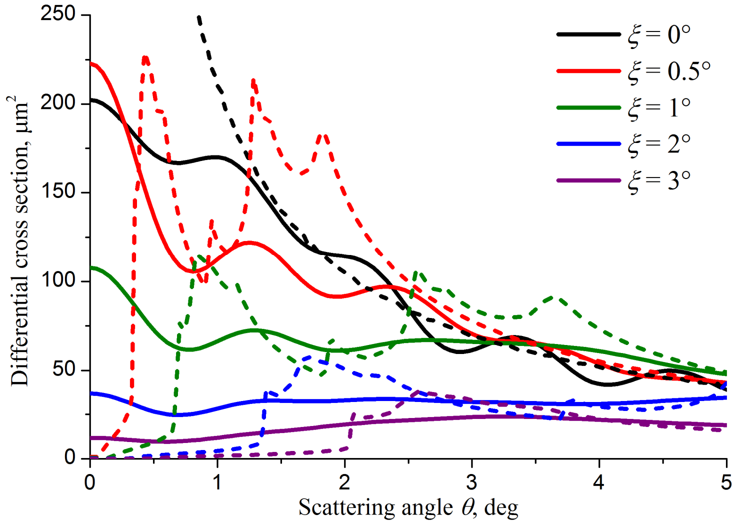

Figure 2. The differential scattering cross sections for the randomly oriented regular and irregular columns calculated in the geometric-optics (dashed) and physical-optics (solid) approximations.

5. BACKSCATTER RATIOS FOR THE RANDOMLY ORIENTED IRREGULAR COLUMNS

The backscattering cross section $\sigma(0)$ for two wavelengths of 0.532 μm and 1.064 μm is shown in Fig. 3(a). We see that there are the distortion angles where the backscattering peak is dissipated at the shorter wavelength and it is not dissipated at the longer wavelength. Consequently, the color ratio increases as it is presented in Fig. 3(b). The linear depolarization ratio presented in Fig. 3(c) also increases with the distortion angle. This increase is explained by the enlargement of the ratio $\sigma_{skw}(0)/\sigma_{str}(0)$ caused by the replacement of the dark interference spot by the bright one. The increasing lidar ratio in Fig. 3(d) results directly from Fig. 3(a).

It is also interesting to note that, for the chosen diameter $D = 30\mu\mathrm{m}$ of the column, the common experimental data of $\delta_l \approx 0.5$, $L \approx 40$, and $\chi \approx 0.8$ are satisfied if we assume that the distortion angle of this column is about $\xi \approx 1°$. Therefore, the data obtained are promising for their applications in practice.

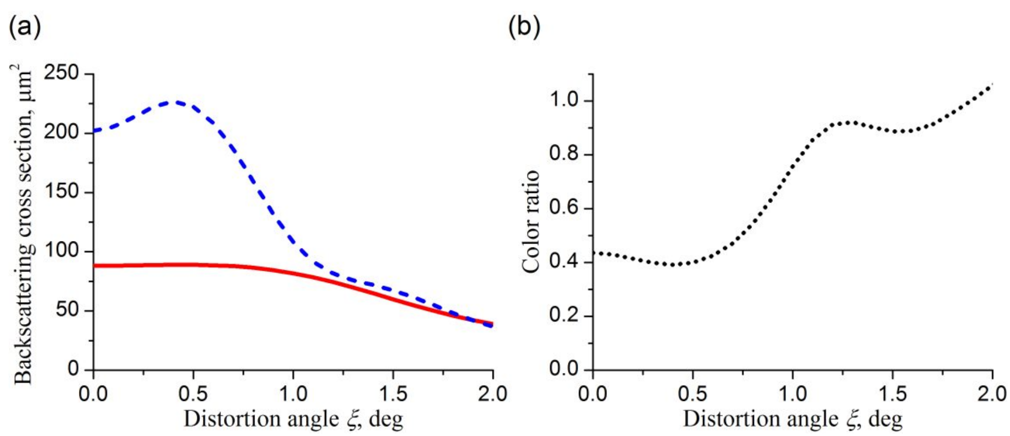

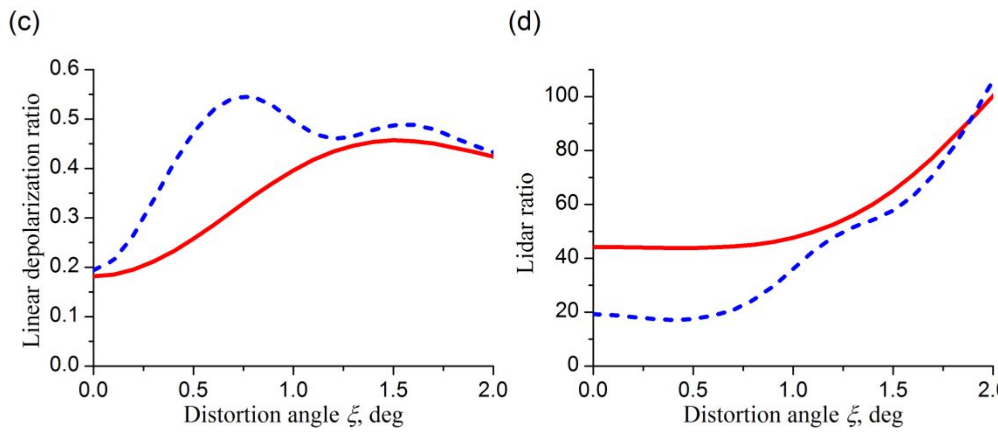

Figure 3. Backscattering cross sections (a) and the backscatter ratios (c-d) for the randomly oriented column versus its distortion angle calculated in the physical-optics approximation for two wavelengths of 0.532 μm (dashed) and 1.064 μm (solid).

6. CONCLUSIONS

In this paper, we have studied the impact of shape distortions of a hexagonal ice column on its backscattering properties at random particle orientation. It is obtained that the backscattering peak around the backward direction previously known for the regular crystal shapes exists for the shape-distorted crystals as well. It spreads from the backward direction until the so-called diffraction angle $\theta_d \approx 3\lambda / D$. However this peak is dissipated for large shape distortions under the condition $\xi > \theta_{dif}$ where ξ is the distortion angle.

Within the backscattering peak, all elements of the Mueller matrix including the differential scattering cross section, as functions of the zenith scattering angle, undergo oscillations with the angular scale of about the interference angle $\theta_{int} \approx \theta_{dif} / 3$. It is proved that these oscillations are caused by interference of four skew beams. Since this interference is sensitive to distortions of the crystal shape, these oscillations are essentially changed with increase of the distortion angle.

The backscatter ratios needed for interpretation of lidar signals are firstly calculated as functions of the distortion angles [32-36]. These results can explain the inconsistencies between the theoretical and experimental data.

ACKNOWLEDGMENTS

This work is supported by the Russian Foundation for Basic Research under Grants no. 15-05-06100 and no. 15-55-53081, by the RF President grant on the support of leading scientific schools NSH-4714.2014.5, by the RF President grant MK-6680.2015.5, by the RF Ministry of Education and Science under the program rising competitiveness of the TSU and supported in part by the Russian Science Foundation (Agreement no. 14-27-00022).

REFERENCES

[1] Shcherbakov, V., Gayet, J. G., Braker, B., and Lawson, P., "Light scattering by single natural ice crystals," J. Atmos. Sci. 63(5), 1513-1525 (2006).
[2] Ulanowski, Z., Hesse, E., Kaye, P. H., and Baran, A. J., "Light scattering by complex ice-analogue crystals," J. Quant. Spectrosc. Radiat. Transf. 100, 382-392 (2006).
[3] Baran, A. J., "A review of the light scattering properties of cirrus," J. Quant. Spectrosc. Radiat. Transf. 110, 1239-1260 (2009).
[4] Cole, B. H., Yang, P., Baum, B. A., Riedi, J., and C.-Labonnote, L., "Ice particle habit and surface roughness derived from PARASOL polarization measurements," Atmos. Chem. Phys. 14, 3739-3750 (2014).
[5] Macke, A., Mueller, J., and Raschke, E., "Single scattering properties of atmospheric ice crystals," J. Atmos. Sci. 53(19), 2813-2825 (1996).

[6] Liu, C., Panetta, R. L., and Yang, P., "The effects of surface roughness on the scattering properties of hexagonal columns with sizes from the Rayleigh to the geometric optics regimes," J. Quant. Spectrosc. Radiat. Transf. 129,169-185 (2013).
[7] Liu, C., Panetta, R. L., and Yang, P., "The effective equivalence of geometric irregularity and surface roughness in determining particle single-scattering properties," Opt. Express 22(19), 23620-23627 (2014).
[8] Sassen, K., and Benson, S., "A midlatitude cirrus cloud climatology from the Facility for Atmospheric Remote Sensing. Part II: Microphysical properties derived from lidar depolarization," J. Atmos. Sci. 58(15), 2103-2112 (2001).
[9] Chen, W.-N., Chiang, C.-W., and Nee, J.-B., "Lidar ratio and depolarization ratio for cirrus clouds," Appl. Opt. 41(30), 6470-6476 (2002).
[10] Hu, Y., Vaughan, M., Liu, Z., Lin, B., Yang, P., Flittner, D., Hunt, B., Kuehn, R., Huang, J., Wu, D., Rodier, S., Powell, K., Trepte, C., and Winker, D., "The depolarization-attenuated backscatter relation: CALIPSO lidar measurements vs. theory," Opt. Express 15(9), 5327-5332 (2007).
[11] Cho, H. M., Yang, P., Kattawar, G. W., Nasiri, S. L., Hu, Y., Minnis, P., Trepte, C., and Winker, D., "Depolarization ratio and attenuated backscatter for nine cloud types: analyses based on collocated CALIPSO lidar and MODIS measurements," Opt. Express 16(6), 3931-3948 (2008).
[12] Reichardt, J., Reichardt, S., Lin, R.-F., Hess, M., McGee, T. J., and Starr, D. O., "Optical-microphysical cirrus model," J. Geophys. Res. 113, D22201 (2008).
[13] Tao, Z., McCormick, M. P., Wu, D., Liu, Z., and Vaughan, M. A., "Measurements of cirrus cloud backscatter color ratio with a two-wavelength lidar," Appl. Opt. 47(10), 1478-1485 (2008).
[14] Okamoto, H., Sato, K., and Hagihara, Y., "Global analysis of ice microphysics from CloudSat and CALIPSO: Incorporation of specular reflection in lidar signals," J. Geophys. Res. 115, D22209 (2010).
[15] Balin, Y. S., Kaul, B. V., Kokhanenko, G. P., and Penner, I. E., "Observations of specular reflective particles and layers in crystal clouds," Opt. Express 19(7), 6209–6214 (2011).
[16] Sassen, K., Kayetha, V. K., and Zhu, J., "Ice cloud depolarization for nadir and off-nadir CALIPSO measurements," Geophys. Res. Lett. 39(20), L20805 (2012).
[17] Hayman, M., Spuler, S., and Morley, B., "Polarization lidar observations of backscatter phase matrices from oriented ice crystals and rain," Opt. Express 22(14), 16976-16990 (2014).
[18] Balin, Yu. S., Kaul, B. V., Kokhanenko, G. P., "Observations of specularly reflective particles and layers in crystal clouds," Optica Atmosfery i Okeana 24(4), 293-299 (2011).
[19] Galileiskii, V. P., Borovoy, A. G., Matvienko, G. G., Morozov, A. M., "Specularly reflected component at light scattering by ice crystals with predominant orientation," Optica Atmosfery i Okeana 21(9), 668-673 (2008).
[20] Galileiskii, V. P., Kaul, B. V., Matvienko, G. G., Morozov, A. M., "Angular structure of the light intensity near the angles of mirror reflection from the faces of ice crystalline particles," Atmospheric and Oceanic Optics 22(5), 506-512 (2009).
[21] Konoshonkin, A. V., Borovoy, A. G., "Specular scattering of light on cloud ice crystals and wavy water surface," Atmospheric and Oceanic Optics 26(5), 438-443 (2013).
[22] Burnashov, A. V., Konoshonkin, A. V., "Matrix of light scattering on a truncated plate-like droxtal preferably oriented in a horizontal plane," Atmospheric and Oceanic Optics 26(3), 194-200 (2013).
[23] Samokhvalov, I. V., Kaul, B. V., Nasonov, S. V., Zhivotenyuk, I. V., Bryukhanov, I. D., "Backscattering matrix of the mirror-reflecting upper-level cloud layers formed by horizontally oriented crystal particles," Optica Atmosfery i Okeana 25(5), 403-411 (2012).
[24] Zhou, C., and Yang, P., "Backscattering peak of ice cloud particles," Opt. Express 23(9), 11995-12003 (2015).
[25] Borovoi, A., Grishin, I., Naats, E., and Oppel, U., "Backscattering peak of hexagonal ice columns and plates," Opt. Lett. 25(18), 1388-1390 (2000).
[26] Borovoi, A. G., Kustova, N. V., and Oppel, U. G., "Light backscattering by hexagonal ice crystal particles in the geometrical optics approximation," Opt. Eng. 44, 071208 (2005).
[27] Borovoi, A. G., and Grishin, I. A., "Scattering matrices for large ice crystal particles," J. Opt. Soc. Am. A 20(11), 2071-2080 (2003).
[28] Borovoi, A., Konoshonkin, A., and Kustova, N., "Backscattering by hexagonal ice crystals of cirrus clouds," Opt. Lett. 38(15), 2881-2884 (2013).
[29] Borovoi, A., Konoshonkin, A., and Kustova, N., "Backscatter ratios for arbitrary oriented hexagonal ice crystals of cirrus clouds," Opt.Lett. 39(19), 5788-5791 (2014).

[30] Sato, K., and Okamoto, H., "Characterization of Ze and LDR of nonspherical and inhomogeneous ice particles for 45-GHz cloud lidar: Its implication to microphysical retrievals," J. Geophys. Res. 111, D22213 (2006).
[31] Mishchenko, M. I., Hovenier, J. W., and Travis, L. D., [Light Scattering by Nonspherical Particles: Theory, Measurements, and Applications], Academic Press, 690 (2000).
[32] Borovoi, A., Konoshonkin, A., and Kustova, N., "The physical-optics approximation and its application to light backscattering by hexagonal ice crystals," J. Quant. Spectrosc. Radiat. Transf. 146, 181-189 (2014).
[33] Konoshonkin, A. V., Kustova, N. V., Borovoy, A. G., "Peculiarities of the depolarization ratio in lidar signals for randomly oriented ice crystals of cirrus clouds," Optica Atmosfery i Okeana 26(5), 385-387 (2013).
[34] Konoshonkin, A. V., Kustova, N. V., Borovoy, A. G., "Beam splitting algorithm for light scattering by atmospheric ice crystals. Part 1. Theory," Optica Atmosfery i Okeana 28(4), 324-330 (2015).
[35] Konoshonkin, A. V., Kustova, N. V., Borovoy, A. G., "Beam splitting algorithm for light scattering by atmospheric ice crystals. Part 2. Comparison with the ray tracing algorithm," Optica Atmosfery i Okeana 28(4), 324-330 (2015).
[36] Konoshonkin, A. V., Kustova, N. V., Borovoi, A. G., "Beam-splitting code for light scattering by ice crystal particles within geometric-optics approximation," J. Quant. Spectrosc. Radiat. Transf., http://dx.doi.org/10.1016/j.jqsrt.2015.06.008 (2015).